

# A new charged particle detector for the KOTO experiment at J-PARC

HongMin KIM for the KOTO Collaboration

Division of Science Education, Jeonbuk National University, Jeonju 54896, Republic of Korea

E-mail: recenter@naver.com

**Abstract.** We installed a new detector called Downstream Charged Veto(DCV) in order to suppress the  $K_L \rightarrow \pi^+\pi^-\pi^0$  decay background for the J-PARC KOTO experiment. Since the background is caused by non-detected charged pions passing through the beam hole of the electromagnetic calorimeter, the detector was installed in vacuum right behind. The DCV is composed of two plastic scintillator pipes read out by Multi Pixel Photon Counter(MPPC)s through wavelength shifting(WLS) fibers. From the test by using cosmic-rays during its fabrication, we obtained about 60 photoelectrons at the center of the DCV is about 60. After its installation, energy calibration was done with cosmic-rays surrounding the  $K_L$  beam, and its signal is identified by detectors surrounding the DCV.

## 1. Introduction

The KOTO experiment at J-PARC is searching for the  $K_L \rightarrow \pi^0\nu\bar{\nu}$  decay, which is one of the most sensitive probes to new physics beyond the standard model(SM). Its signature is a pair of photons from a  $\pi^0$  decay without any additional activity in a hermetic detector system surrounding the decay region. To detect this highly suppressed decay, expected at the  $3 \times 10^{-11}$  level, it is important to reject background events related to other kaon decay modes. At the single event sensitivity of  $1.30 \times 10^{-9}$  achieved by data collected in 2015, the number of  $K_L \rightarrow \pi^+\pi^-\pi^0$  background was estimated as  $0.05 \pm 0.02$  which corresponds to 2 at the SM sensitivity. According to a Monte Carlo(MC) simulation, as shown in Fig. 1,  $\pi^+$  and  $\pi^-$  coming through the beam hole in the electromagnetic calorimeter made of CsI and the beam pipe downstream of it could interact with non-active materials such as the Al beam pipe and a G10 pipe inside.

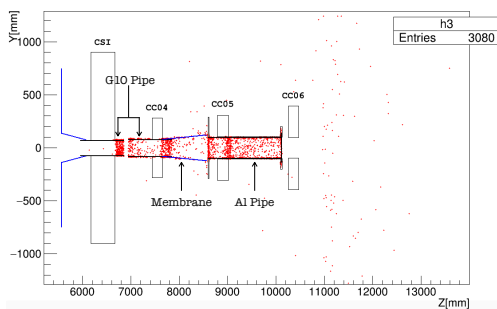


**Figure 1.** Interacting point with  $\pi^+$  and  $\pi^-$ . Red dots indicate where the charged pions disappeared. The membrane is thin files to separate the high-vacuum region and the low-vacuum region. The G10 pipes support the membrane.

21 To reduce the  $K_L \rightarrow \pi^+\pi^-\pi^0$  background events, we have to detect the charged pions  
 22 before they interact with non-active materials. For the purpose, we decided to install a new  
 23 charged particle detector, DCV, inside a high vacuum region downstream of the electromagnetic  
 24 calorimeter. To minimize the non-detected area, the DCV is placed as close as possible to the  
 25 electromagnetic calorimeter.

## 26 2. Scheme of the DCV

27 The DCV consists of two square pipes with 4 sheets of scintillators combined. The DCV1 is  
 28 located inside the membrane with the CC04, and the DCV2 is located inside the aluminum  
 29 beam pipe. The G10 pipe at the CsI was shortened from 900 mm to 550 mm, and the G10 pipe  
 30 at the CC04 was removed. The scheme of the DCV is shown in Fig. 2. One module of the  
 31 DCV consists of a 5-mm-thick plastic scintillator(EJ200, Eljen Technology) with 18 embedded  
 32 WLS fibers(Y-11(200M), Kuraray). The diameter of WLS fiber is 1 mm. Due to very limited  
 33 space for the DCV, we evaluated the new scheme of the light collection. In the new scheme of  
 34 the light collection, the 4 MPPCs are directly attached to the surface of the scintillator through  
 35 the light guide made of aluminum which is placed in the scintillator. The WLS fibers in the  
 36 grooved scintillator are routed into the light guide. In this design, the WLS fibers are naturally  
 37 bent to converge into the light guide. Figure 3 shows the light loss due to the curvature of the  
 38 WLS fiber. We measured the light yield by MPPC of the LED light(430 nm) passing through  
 39 the bent fiber. The light loss increases rapidly if the radius is less than 20 mm.

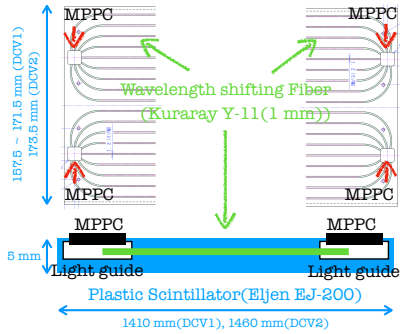


Figure 2. Scheme of the DCV.

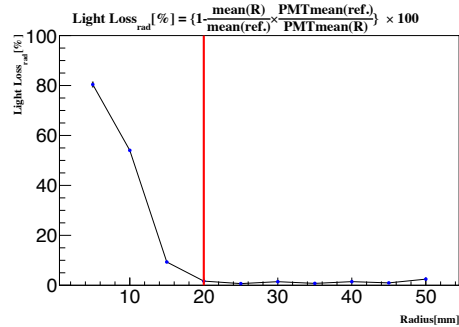


Figure 3. The light loss due to the curvature of the WLS fiber. The radius is a parameter of curvature.

## 40 3. Fabrication Process

### 41 3.1. MPPC Gain Measurement and Fiber Test

42 The 4 MPPCs belonging to each scintillator plate were applied the same operating voltage.  
 43 To group the MPPCs into four similar gain sets, we measured the MPPC (S13360-6050PE,  
 44 Hamamatsu)s single-photon gain using the LED light(430 nm). We also measured the light yield  
 45 of the WLS fibers. The LED light(430 nm) was injected on one side of the flagged WLS fiber  
 46 that we assigned before, and the MPPC was attached on the other side. After the measurement  
 47 of the light yield, we chose the WLS fiber with a high light yield.

### 48 3.2. Making the scintillator pipe

49 First, the WLS fibers were glued to the plastic scintillator using the optical cement(BC-600,  
 50 Saint-Gobain). The scintillators were dried for at least 48 hours. Second, the scintillators were  
 51 placed in a vacuum chamber. We extracted the outgas from the glued scintillators at less than

52 1 Pa, over 48 hours. Third, the scintillators were wrapped by a 12- $\mu\text{m}$ -thick aluminized film.  
 53 Next, the MPPCs were respectively attached on the light guide and fixed by aluminum plates.  
 54 After the cosmic-ray test, the scintillators were assembled to a square pipe.

### 55 3.3. Cosmic-ray test

56 To evaluate the light yield of the DCV, we measured the number of p.e. using cosmic-rays at  
 57 8 points, as shown in Fig. 4. At the center, the average number of p.e. for 1 MeV was 60.2  
 58 for the DCV1 and 58.6 for the DCV2. By fitting the data with an exponential function, the  
 59 attenuation length was found to be  $2469 \pm 165.1$  mm for the DCV1 and  $2566 \pm 166.0$  mm for  
 60 the DCV2.

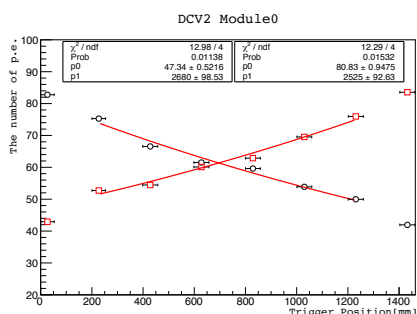


Figure 4. The number of p.e. at each cosmic-ray trigger point

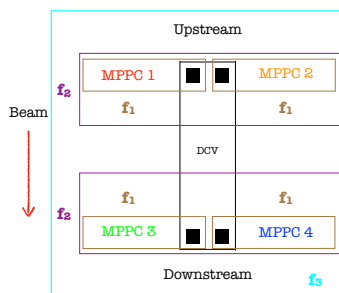


Figure 5. Calibration method for the DCV with 4 MPPCs. There are 3 types of normalization factors ( $f_1$  : for each MPPC,  $f_2$  : for a pair of MPPC at upstream(downstream),  $f_3$  : for all MPPCs).

## 61 4. Energy Calibration

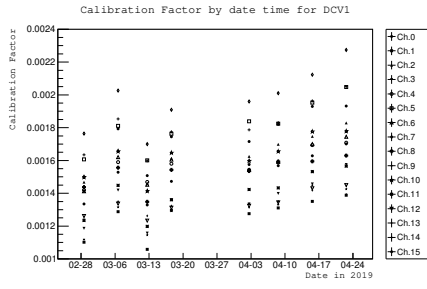
62 After the installation of the DCV in the KL beamline, we took the cosmic-ray data for an  
 63 energy calibration. The CC04 and CC05 surrounding the DCV were used as the trigger counter.  
 64 Figure 5 shows the diagram of the calibration method for the DCV with 4 MPPCs which were  
 65 shared one energy deposit. The energy response to the cosmic-ray of each module of the DCV  
 66 was used to derive the 3 types of normalization factors. Each normalization factor was obtained  
 67 from MIP peak by fitting the pulse height distribution. During the beam time from Feb. to  
 68 Apr. 2019, we collected the cosmic-ray data. Figure 6 shows how the calibration factor varies  
 69 during the period. The calibration factors tend to increase over time.

## 70 5. Summary

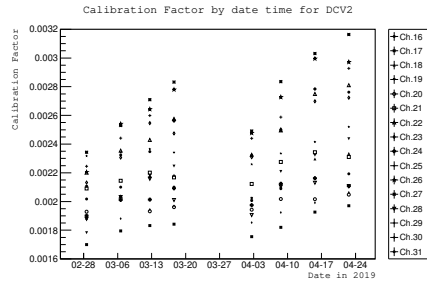
71 We fabricated and installed a new charged particle detector, the DCV, for further rejection of  
 72 the background events from the  $K_L \rightarrow \pi^+\pi^-\pi^0$  decay. Based on the cosmic-ray test performed  
 73 during its fabrication, the light yield is about 60 p.e. for 1 MeV at the center of the DCV. We  
 74 established a method of its calibration by using cosmic-ray identified by detectors surrounding  
 75 the DCV. The energy calibration was done for the MeV scale. Studies on stability of its  
 76 performance during the beam time is undergoing.

## 77 Acknowledge

78 This work is supported by the National Research Foundation of Korea-2017R1A2B4006359,  
 79 and the JSPS KAKENHI Grant No. JP23224007.



(a)



(b)

**Figure 6.** Calibration Factor over time for DCV1(a) and DCV2(b).

80 **Reference**

- 81 [1] J.K. Ahn *et al.* (KOTO Collaboration) 2019, *Phys. Rev. Lett.* **122** 021802